Adsorption States of NO_2 over Water−Ice Films Formed on Au(111)

Shinri Sato,*,† Dai Yamaguchi,† Kikuko Nakagawa,† Yoshihiko Inoue,‡ Akihiro Yabushita,‡ and Masahiro Kawasaki‡

Catalysis Research Center and Graduated School of Environmental Earth Science, Hokkaido University, Sapporo 060-0811, Japan, and Department of Molecular Engineering, Kyoto University, Kyoto 606-8501, Japan

Received May 1, 2000. In Final Form: July 19, 2000

The adsorption states of NO_2 over amorphous and crystalline water−ice films formed on an Au(111) surface have been studied in an ultrahigh vacuum system by the temperature programmed desorption (TPD) technique and IR absorption−reflection spectroscopy (IRAS). The ice films are prepared by deposition of gas phase water on the Au substrate at <100 K for amorphous ice and at 140 K for crystalline ice. The surface of amorphous ice is characterized by the high density of free OH, while that of crystalline ice is characterized by grain boundaries and the lack of free OH. TPD for pure ice shows only one desorption peak of H_2O, while after NO_2 adsorption on it an additional weak H_2O desorption peak appears at 185 K. This higher-temperature peak is attributable to decomposition of NO_2−H_2O adducts. IRAS measurements revealed that NO_2 adsorbs on ice surfaces as N_2O_4 with D_{2h} symmetry and that neither N_2O_4 isomers such as D-isomers nor NO_x (x = 1, 2, and 3) species are produced in the temperature range of 90−140 K. Interaction of the ice surfaces with NO_2 (N_2O_4) as well as orientation of N_2O_4 adsorbed on the ice surfaces are investigated as a function of temperature. Thermal decomposition of NO_2 adsorbed on the water−ice formed on an Au surface is reconfirmed, which has been reported by Wang and Koel (*J. Phys. Chem. A* **1998**, *102*, 8573). A possible mechanism for the NO_2 decomposition is proposed.

1. Introduction

Heterogeneous reactions on water−ice particles have attracted attention in atmospheric chemistry. Polar stratospheric clouds, which consist of nitric acid trihydrate (type I PSC) and water−ice (type II PSC), have been implicated as playing a central role in the photochemical mechanism responsible for the yearly occurrence of the ozone hole.[1−3] Thus, a study of molecular adsorption on condensed water surfaces is important from an environmental chemistry point of view. We have recently studied the photodissociation dynamics of N_2O_4 adsorbed on amorphous and crystalline water−ice films at 80−140 K using 193, 248, and 351 nm laser light.[4] We found that the photodissociation yield at 193 nm is much higher on amorphous ice than on crystalline ice. We assume that the large difference in the photodissociation yield between both ice film structures is due to a difference in the adsorption states of N_2O_4 on the ice films. Wang and Koel,[5,6] on the other hand, reported thermal decomposition of NO_2 coadsorbed with water−ice on an Au(111) surface during TPD. This decomposition produces atomic oxygen on the Au surface, which desorbs at 510 K. They ascribed the NO_2 decomposition to the formation of D-isomers, ONO−NO_2, and nitrosonium nitrate, $NO^+NO_3^-$, in the interface region between amorphous ice and the N_2O_4 layer.

A thin water−ice film has been used as a model surface for type II PSC, because it can be prepared on various solid materials and facilitates sensitive spectroscopic methods to assign chemical species on the surfaces.[7−19] Especially, when a reflective metal is used as a substrate, IR reflection absorption spectroscopy (IRAS) and temperature-programmed desorption (TPD) techniques are utilized for characterization of water−ice surfaces as well as for analysis of adsorbates on the surface.[15−19] Since IRAS has the surface selection rule, orientation of adsorbates can be determined.[20,21] In the present study, we have investigated interactions of NO_2 with amorphous and crystalline water−ice films formed on an Au(111)

* E-mail: shinri@cat.hokudai.ac.jp. Fax: +81-11-709-4748.
† Hokkaido University.
‡ Kyoto University.

(1) Solomon, S.; Garcia, R. R.; Rowland, F. S.; Wuebbles, D. J. *Nature* **1986**, *321*, 755.
(2) Toon, O. B.; Turco, R. P. *Sci. Am.* **1991**, *264*, 68.
(3) Toon, O. B.; Tolbert, M. A. *Nature* **1995**, *375*, 218.
(4) Yabushita, A.; Inoue, Y.; Senga, T.; Kawasaki, M.; Sato, S. *J. Chem. Phys. B*, submitted.
(5) Wang, J.; Voss, M. R.; Busse, H.; Koel, B. E. *J. Phys. Chem. B* **1998**, *102*, 4693.
(6) Wang, J.; Koel, B. E. *J. Phys. Chem. A* **1998**, *102*, 8573.
(7) Tolbert, M. A.; Middlebrook, A. M. *J. Geophys. Res.* **1990**, *95*, 22423.
(8) Middlebrook, A. M.; Tolbert, M. A. *Geophys. Res. Lett.* **1996**, *23*, 2145.
(9) Koehler, B. G.; Middlebrook, A. M.; Tolbert, M. A. *J. Geophys. Res.* **1992**, *97*, 8065.
(10) Kehler, B. G.; McNeil, L. S.; Middlebrook, A. M.; Tolbert, M. A. *J. Geophys. Res.* **1993**, *98*, 10563.
(11) Middlebrook, A. M.; Iraci, L. T.; McNeil, L. S.; Koehler, B. G.; Wilson, M. A.; Saastad, O. W.; Tolbert, M. A. *J. Geophys. Res.* **1993**, *98*, 20473.
(12) Middlebrook, A. M.; Berland, B. S.; Georg, S. M.; Tolbert, M. A. *J. Geophys. Res.* **1994**, *99*, 25655.
(13) Graham, J. D.; Roberts, J. T. *Geophys. Res. Lett.* **1995**, *22*, 251.
(14) Graham, J. D.; Robert, J. T. *J. Phys. Chem.* **1994**, *98*, 5974.
(15) Horn, A. B.; Banham, S. F.; McCoustra, M. R. S. *J. Chem. Soc., Faraday Trans.* **1995**, *91*, 4005.
(16) Horn, A. B.; Koch, T.; Chester, M. A.; McCoustra, M. R. S.; Sodeau, J. R. *J. Phys. Chem.* **1994**, *98*, 946.
(17) Koch, T. G.; Banham, S. F.; Sodeau, J. R.; Horn, A. B.; McCoustra, M. R. S.; Chesters, M. A. *J. Geophys. Res.* **1997**, *102*, 1513.
(18) Rieley, H.; McMurray, D. P.; Haq, S. *J. Chem. Soc., Faraday Trans.* **1996**, *92*, 933.
(19) Rieley, H.; Colby, D. J.; McMurray, D. P.; Reeman, S. M. *J. Phys. Chem. B* **1997**, *101*, 4982.
(20) Greenler, R. G.; Rahn, R. R.; Schwartz, J. P. *J. Catal.* **1971**, *23*, 42.
(21) Suetaka, W. *Surface Infrared and Raman Spectroscopy*; Prenum Press: New York and London, 1995; p 13.

10.1021/la000628n CCC: $19.00
Published on Web 11/02/2000

surface, examining the adsorption states of NO_2 and precursor states for the NO_2 decomposition.

2. Experimental Section

All the experiments were carried out in an ultrahigh vacuum system (base pressure, 2×10^{-10} Torr), details of which were described previously.[22,23] An Au(111) single crystal (10 mm in diameter) used as a substrate was cleaned by repeating cycles of Ar-ion sputtering and annealing at 800 K, followed by oxidation with O_3. Thermal desorption spectra (TDS) of adsorbates were obtained with a quadrupole mass spectrometer (ANELVA AQA-200), which was located at ~35° with respect to the substrate surface normal. For IRAS measurements, the IR beam from FTIR (BIO-RAD FTS-155) was focused by a BaF_2 lens onto the sample in the chamber through a BaF_2 window, the cutoff wavelength of which is ~900 cm^{-1}. The incident angle of the IR beam was ~85°. A wire grid polarizer was used to select p-polarized light, since only p-polarized light is effective for IRAS.[20,21] The paths of the IR beam were purged with dry air to reduce the effects of moisture. IRA spectra were recorded with 4 cm^{-1} resolution and 200 scans.

Water used was ultrapure Millipore water and outgassed by repeating a freeze−pump−thaw cycle. The reservoir of water was immersed in a water−ice mixture bath during experiments to keep its vapor pressure constant. NO_2 was stored in a glass reservoir in the presence of an excess of O_2 to prevent its decomposition to NO and O_2 during storage. The gas mixture was frozen at 77 K, and O_2 was pumped away before use. Since NO_2 was decomposed to some extent in the gas handling system, the inner wall of the stainless steel tube was passivated by exposing a relatively high pressure of NO_2 or O_3 for a prolonged time. Gases were introduced into the chamber through a nozzle, the end of which was ~1 cm away from the substrate. A pulsed valve (General Valve) was used to control exposures of gases. The NO_2 exposure necessary for a monolayer coverage (1 ML) of chemisorbed NO_2 on an Au(111) surface was determined previously at 160 K,[23] and the same exposure−coverage relation was applied for ice surfaces. Therefore, a real coverage for an amorphous ice surface could be different from the coverage indicated, since a roughness factor of the amorphous ice surface would be greater than unity.

3. Results and Discussion

3.1. Characterization of Water−Ice Films on Au(111). The desorption temperature of H_2O from an Au(111) surface is raised from 150 to 160 K as H_2O coverage increases. This result is in agreement with a previous result for H_2O/Au(111).[24] IRA spectra of H_2O adsorbed on an Au(111) surface at 93 K are shown in Figure 1. The IRAS bands of a thin ice film have been assigned previously.[16,18] The sharp band at 3700 cm^{-1} is assigned to the stretching of free or dangling OH at the ice surface, the broad and strong band at 3389 cm^{-1} to OH stretching in bulk ice, and the weak band at 1654 cm^{-1} to HOH bending in bulk ice. The spectrum closely resembles the IR transmission spectrum of a water film at room temperature except for the 3700 cm^{-1} band,[25] indicating that the ice film on Au(111) is an amorphous ice layer.

When an ice film was formed at <100 K and then heated, a significant change in the IRAS spectrum was observed, as shown in Figure 2. The bulk OH stretching band shifts to lower frequencies by >100 cm^{-1} at 140 K, while the bands of the free OH stretch and the HOH bend decrease in intensity. The spectrum at 140 K is basically identical

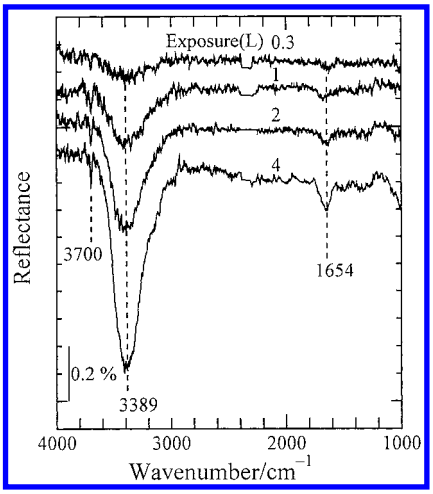

Figure 1. IR reflection absorption (IRA) spectra of H_2O adsorbed on an Au(111) surface at 93 K as a function of exposure.

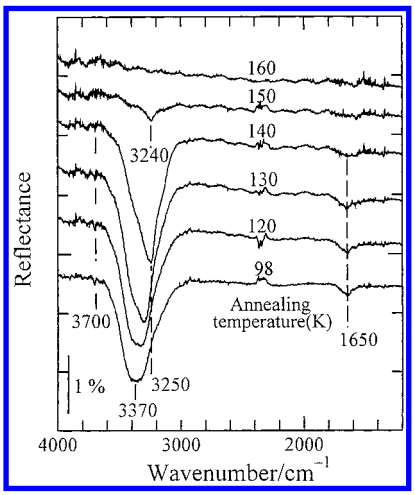

Figure 2. Temperature dependence of the IRA spectrum of H_2O adsorbed on an Au(111) surface. H_2O was first adsorbed at 98 K, and then the substrate was heated stepwisely to the indicated temperatures.

to that of crystalline ice.[7] Since these spectral changes start at 120 K, the phase change of amorphous ice to crystalline ice occurs at >120 K. Thus, an amorphous ice film was prepared by deposition of gas-phase water on Au(111) at <100 K. A crystalline ice film was prepared by H_2O deposition at 140 K, followed by annealing at the same temperature for 10 min. Complete crystallization of the ice film deposited at 130 K needed >25 min of annealing at the same temperature. When the ice film was deposited at 130 K and annealed at the same temperature for 10 min, we refer to this film as a semicrystalline ice film.

The degree of ice crystallinity was found to depend on ice coverage. With decreasing amorphous ice coverage, growth of the bulk OH band of crystalline ice upon 130 K annealing becomes indiscernible, as shown in Figure 3. This result implies that the thinner ice film on an Au(111) surface is hardly crystallized, in agreement with a recent STM study on H_2O/Au(111),[26] which shows water first adsorbs as a planar, amorphous, monolayer-high film.

Since TDS from H_2O/Au(111) show no transient features with increasing H_2O coverage from monolayer to multilayer,[24] it is difficult to determine the monolayer coverage of the ice film from the TPD results alone. In the present

(22) Sato, S.; Suzuki, T. *J. Phys. Chem.* **1996**, *100*, 14769.
(23) Sato, S.; Senga, T.; Kawasaki, M. *J. Phys. Chem. B* **1999**, *103*, 5063.
(24) Kay, B. D.; Lykke, K. R.; Creighton, J. R.; Ward, S. J. *J. Chem. Phys.* **1989**, *91*, 5120.
(25) Ataka, A.; Yotsuyanagi, T.; Osawa, M. *J Phys. Chem.* **1996**, *100*, 10664.
(26) Ikeyama, N.; Gewirth, A. A. *J. Am. Chem. Soc.* **1997**, *119*, 9919.

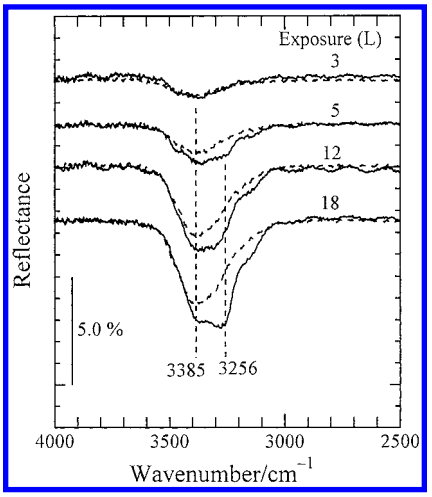

Figure 3. Coverage dependence of the crystallization of amorphous ice adsorbed on an Au(111) surface. H_2O was first adsorbed at 90 K (dotted line), followed by annealing at 130 K for 10 min (solid line).

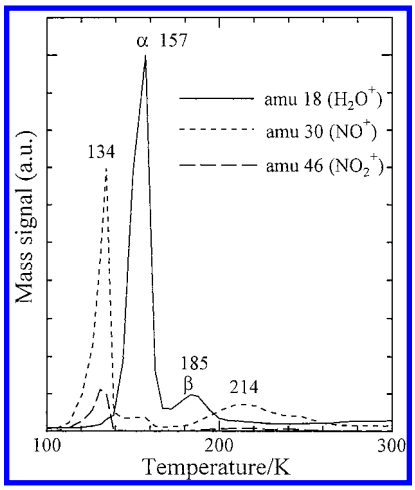

Figure 4. TDS from NO_2 adsorbed on amorphous ice. The temperature ramp was 4 K s^{-1}.

study, we define the monolayer coverage of H_2O/Au(111) as a maximum coverage at which ice crystallization does not occur at 130 K. We estimated the H_2O exposure necessary for 1 ML to be ~3 L (1 L = 1 × 10^{-6} Torr s).

3.2. Adsorption States of NO_2 on Water−Ice Films. Figure 4 shows TDS of NO^+, NO_2^+, and H_2O^+ from NO_2 adsorbed on amorphous ice. The spectra for NO_2^+ and NO^+ are very similar to those from NO_2/Au(111).[6,23,27] The peak centered at 134 K is attributed to physisorbed N_2O_4, and the peak centered at 214 K to NO_2 chemisorbed on the Au surface (chemisorbed NO_2). Since chemisorbed NO_2 is not observed by IRAS at the initial stage of TPD, as will be described later, the presence of the chemisorbed NO_2 peak indicates that part of the N_2O_4 adsorbed on the ice surface is held in the bulk of ice and then moves onto the Au surface upon heating. TDS for H_2O exhibit two desorption peaks in this case. The lower temperature peak (α peak) is identical to that from H_2O/Au(111), and the higher temperature peak (*β* peak) is due to interaction of ice with NO_2, that is, adduct formation. The *β* peak is thus related to the formation of chemisorbed NO_2 on an Au surface. TDS from NO_2 adsorbed on crystalline ice showed very similar features to what was observed for amorphous ice. The fact that the *β* peak was observed for both amorphous and crystalline ice suggests that interaction of free OH with NO_2 is not related with formation of the NO_2−H_2O adduct.

Parts a and b of Figure 5 show IRA spectra of NO_2 adsorbed on crystalline and semicrystalline ice, respectively, as a function of NO_2 exposure. The assignments of IRAS bands for NO_2 adsorbed on a water−ice film were reported by Rieley et al.:[18] the bands at ~1300 cm^{-1} and the bands at ~1750 cm^{-1} are attributed to the ONO symmetric stretching and the ONO asymmetric stretching of N_2O_4 with D_{2h} symmetry, respectively. Similarly to their results, the complete absence of the strong asymmetric stretching band of NO_2 at 1600−1650 cm^{-1} in Figure 5 indicates the absence of NO_2 monomer as well as D-isomers, O═N−O−NO_2. When N_2O_4 coverage exceeds 4 ML, the band at 1180 cm^{-1} becomes discernible for crystalline ice, as shown in Figure 5a. This band is attributable to the ONO symmetric stretching of NO_2 adsorbed directly on the Au surface (chemisorbed NO_2). The formation of chemisorbed NO_2 implies that NO_2 or N_2O_4 can reach the Au surface through grain boundaries of crystalline ice. The result that the 1180 cm^{-1} band can be seen when N_2O_4 coverage exceeds 5 ML would be due to the time required for N_2O_4 to pass through the ice film, since the IRAS spectrum was recorded as N_2O_4 coverage was increased stepwisely. The ice coverage through which NO_2 can reach the Au surface was estimated to be <10 ML for crystalline ice. IRA spectra of N_2O_4 on semicrystalline ice are basically identical with those for crystalline ice, but both the ONO symmetric and the ONO asymmetric stretching bands become broader than those for crystalline ice. This band broadening may be ascribed to the appearance of new adsorption states caused by interaction of N_2O_4 with a semicrystalline ice surface. Semicrystalline ice also has grain boundaries, the depth of which is ~4 ML thickness.

IRAS is selectively sensitive to the vibrational modes perpendicular to a surface (surface selection rule),[20,21] and therefore, we can obtain information about molecular orientation with respect to a metal surface. Figure 6 illustrates three orientations of N_2O_4 adsorbed on a surface. For orientation a, the ONO symmetric stretching parallel to the N−N bond axis is IRAS active but not the ONO asymmetric stretching. On the contrary, for orientation b, the asymmetric stretching perpendicular to the surface is IRAS active but not the symmetric stretching. For orientation c, both the vibrational modes are IRAS inactive. If the orientation of N_2O_4 adsorbed on a flat ice surface over a metal is determined, then information about three-dimensional configurations of a rough ice surface may be obtained from the IRA spectrum of adsorbed N_2O_4.

In Figure 5a and b, the band at ~1266 cm^{-1} was ascribed by Rieley et al.[18] to the ONO symmetric stretching of the first-layer N_2O_4 on the ice surface and has an intensity comparable to that of the ONO asymmetric stretching bands. Since an IR transmission spectrum of gas phase N_2O_4 exhibits both the symmetric and asymmetric ONO stretching bands in comparable intensities, the first-layer N_2O_4 should be randomly oriented. For crystalline ice of Figure 5a, the first-layer N_2O_4 bands in the symmetric and asymmetric ONO stretching regions grow slowly with increasing NO_2 exposure, and the growth stops virtually at ~5 ML. At the same time, the sharp band at 1297 cm^{-1} grows rapidly and becomes dominant at >5 ML. These results indicate that the formation of a disordered N_2O_4 layer is actually limited in the first 5 ML and that ordered N_2O_4 in orientation a of Figure 6 dominates in multilayers over 5 ML, provided that the surface of crystalline ice is flat and parallel to the Au surface. Since a randomly oriented N_2O_4 layer is less than 5 ML on the NO_2-covered

(27) Bartram, M. E.; Koel, B. E. *Surf. Sci.* **1989**, *213*, 137.

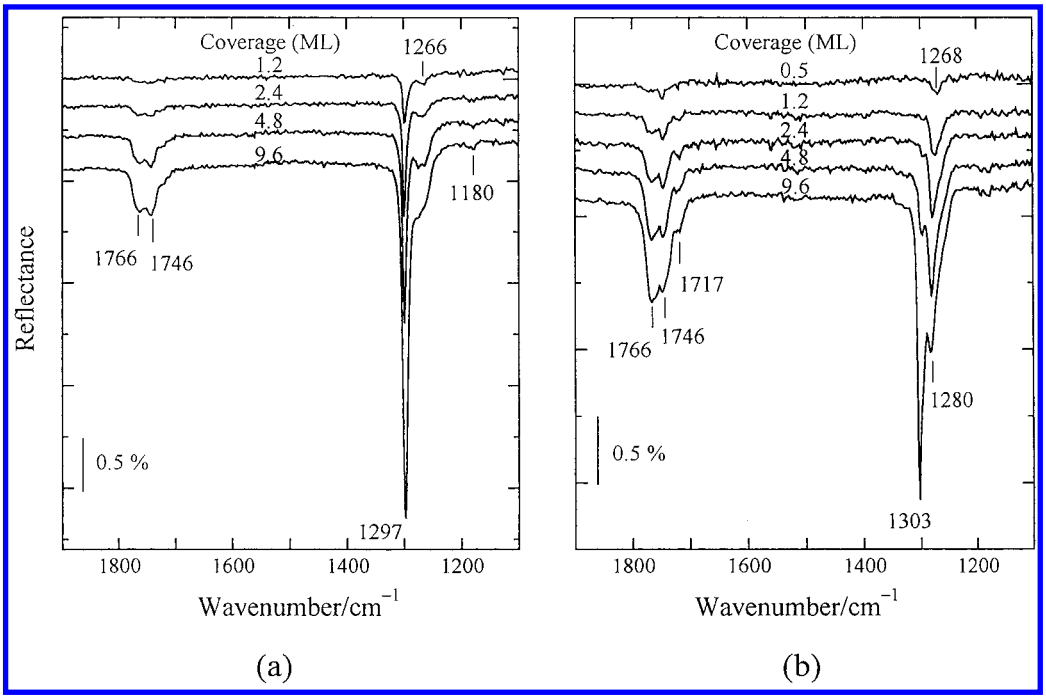

Figure 5. IRA spectra of N_2O_4 adsorbed at 91 K as a function of N_2O_4 coverage on (a) 8 ML crystalline ice and (b) 5 ML semicrystalline ice.

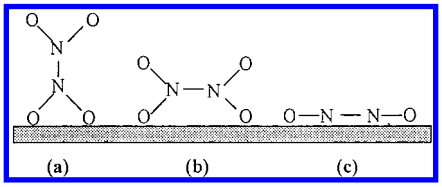

Figure 6. Orientations of N_2O_4 adsorbed on a surface.

Au(111) surface,[23] the crystalline ice surface may not be completely flat.

N_2O_4 adsorbed on semicrystalline ice shows a more complicated IRAS spectrum than that on crystalline ice, so that we applied curve fitting to analyze the spectra in Figure 5b on the assumption that the IRAS absorbance band shape is Lorentzian. The results show that the ONO symmetric stretching region consists of four bands typically at 1303, 1298, 1280, and 1266 cm^{-1}. The sharp bands at 1303 and 1298 cm^{-1} show a similar dependence on N_2O_4 coverage. Since the 1303 cm^{-1} band exhibits a much sharper bandwidth than the 1298 cm^{-1} band, the species giving the 1303 cm^{-1} band would be relatively free. We tentatively assign the 1298 cm^{-1} band to N_2O_4 in a multilayer N_2O_4 lattice and the 1303 cm^{-1} band to N_2O_4 just outside the lattice or in a loose lattice, both of which are in orientation a. The N_2O_4 species giving the 1280 cm^{-1} band is not observed for crystalline ice and, therefore, would interact strongly with the ice surface, but further detailed features of this species are not understood well at present. The curve fitting analysis for adsorbed N_2O_4 is still under progress, and its details will be reported elsewhere.

When NO_2 was adsorbed on amorphous ice, its IRA spectra are basically similar to those for semicrystalline ice, as shown in Figure 7b. The frequencies, intensities, and assignments of N_2O_4 adsorbed on the ice surfaces are summarized in Table 1. The chemisorbed NO_2 band was not observed even for 1 ML amorphous ice coverage, indicating that amorphous ice is continuous and has no grain boundaries. Although various kinds of NO_2 species are formed in a low-temperature inert gas matrix[28] and on solid substrates,[29−33] NO_2 adsorption on amorphous and crystalline ice results in formation of a pure N_2O_4 layer. Also, D-isomers, nitrosonium nitrate, and HONO were not detected on any ice films used. It should be noted that failure in detecting D-isomers and nitrosonium nitrate is not due to insufficient sensitivity of IRAS, since these species have been detected by IRAS previously.[29−33]

After NO_2 adsorption on semicrystalline and amorphous ice at ~90 K, the substrate temperature was elevated to examine a change in the adsorption states of N_2O_4. Figure 8 shows a significant difference in temperature dependence between amorphous and semicrystalline ice. For N_2O_4 adsorbed on semicrystalline ice, the 1303 cm^{-1} band rapidly increases in intensity with increasing temperature with a band shift to lower frequencies, while the bands in the ONO asymmetric stretching region decrease. Curve fitting analysis revealed that the 1303 cm^{-1} band merges into the 1298 cm^{-1} band at 110 K, forming a sharp band at 1296 cm^{-1}. We assume that relatively free N_2O_4 in orientation a is involved in a well-ordered N_2O_4 lattice at >110 K. The 1280 cm^{-1} band grows with elevating temperature up to 120 K, while the 1266 cm^{-1} band remains virtually unchanged. The growth of the 1280 cm^{-1} band seems to be related to the decrease of the asymmetric stretching bands. Therefore, randomly ordered N_2O_4 may convert to some extent into ordered N_2O_4, giving the 1280 cm^{-1} band. For the amorphous ice case shown in Figure 7b, both the symmetric and asymmetric stretching bands increase in intensity at higher temperatures. It was shown by curve fitting that the 1302 cm^{-1} band also merges into the 1298 cm^{-1} band at 120 K, and the latter shifts significantly to lower frequencies at >100 K. The 1280 cm^{-1} band decreases to some extent at 120 K, but the

(28) Bandow, H.; Akimoto, H.; Akiyama, S.; Tezuka, T. *Chem. Phys. Lett.* **1984**, *111*, 496.
(29) Fateley, W. G.; Bent, H. A.; Crawford, B., Jr. *J. Chem. Phys.* **1939**, *31*, 204.
(30) Hisatsune, I. C.; Devlin, J. P.; Wada, Y. *J. Chem. Phys.* **1960**, *33*, 714.
(31) Varetti, E. L.; Pimentel, G. C. *J. Chem. Phys.* **1971**, *55*, 3813.
(32) Givan, A.; Loewenschuss, A. *J. Chem. Phys.* **1989**, *90*, 6135.
(33) Givan, A.; Loewenschuss, A. *J. Chem. Phys.* **1989**, *91*, 5126.

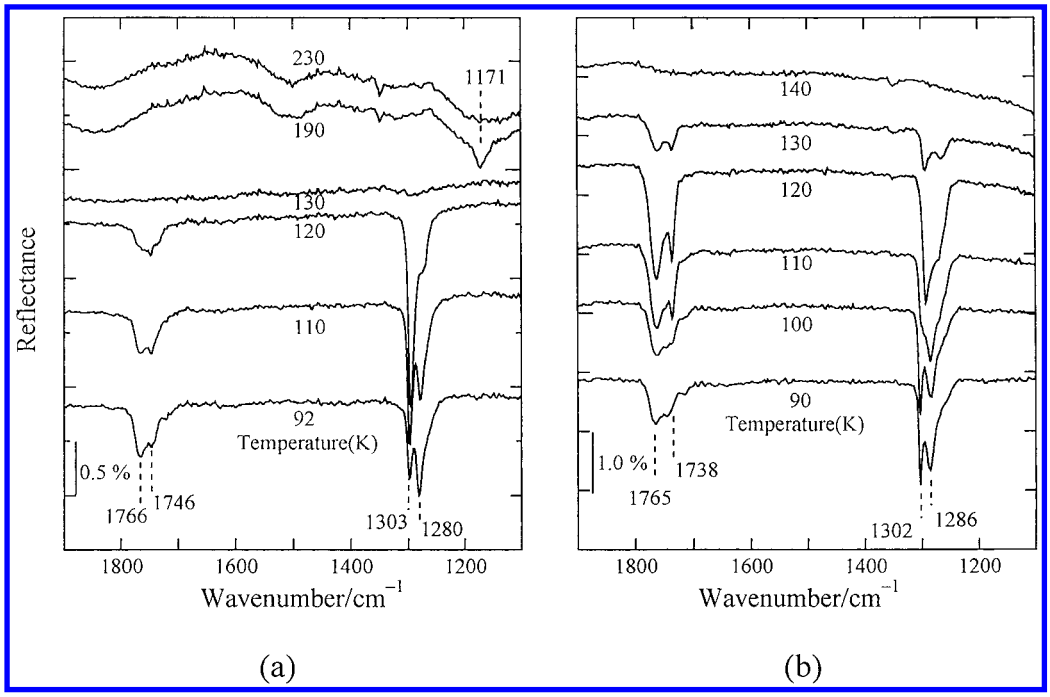

Figure 7. Temperature dependence of the IRA spectrum of N_2O_4 adsorbed on (a) 5 ML semicrystalline ice and (b) 3 ML amorphous ice. The substrate temperature was elevated stepwisely to the indicated temperatures.

Table 1. Vibrational Frequencies and Tentative Assignments of N_2O_4 (D_{2h}) Adsorbed on Water−Ice Surfaces at ~2.4 ML

band (cm^{-1})	intensities[a] crystalline ice	semicrystalline ice	amorphous ice	tentative assignments[b]
		ν_{ssym} Region		
1256	none	none	W	D
1266−1271	W	W	W	B
1278−1285	none	M	S	C
1290−1303	S	W	S	A
		ν_{assym} Region		
1712−1716	none	W	M	C
1735	none	none	M	D
1745−1746	W	M	S	B
1761−1772	W	M	S	B

[a] S, strong; M, medium; W, weak; VW, very weak. [b] A, N_2O_4 in a lattice or a loose lattice; B, randomly oriented N_2O_4; C, N_2O_4 interacted with the ice surface; D, N_2O_4 interacted strongly with the amorphous ice surface.

1266 cm^{-1} band grows significantly at 120 K. These results are explained as follows: the multilayer N_2O_4 is crystallized and undergoes strong interaction with interlayer N_2O_4 at >100 K, and the species giving the 1280 cm^{-1} band partly converts into disordered N_2O_4 at 120 K. In addition, the increase in the total area of the symmetric stretching as well as the asymmetric stretching bands upon heating indicates that IRAS inactive species become IRAS active species at higher temperatures. As described below, amorphous ice has much higher densities of free OH and loosely bound H_2O molecules than crystalline ice. The surface of amorphous ice is known to interact strongly with compounds having hydrogen bond donors.[36] Such a reactivity of amorphous ice may produce various adsorption states of N_2O_4 on its surface. We also examined carefully if D-isomers and/or $NO^+NO_3^-$ are formed on amorphous ice at elevated temperatures, since Givan and Lowenschuss[33] reported that $NO^+NO_3^-$ is produced by

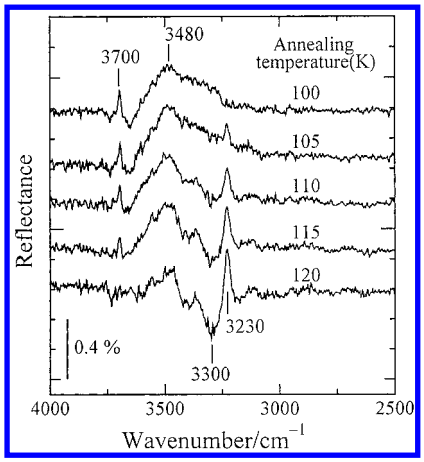

Figure 8. Difference spectra in the OH stretching region upon NO_2 adsorption on amorphous ice, followed by annealing at the indicated temperatures. The spectra are referred to that taken for pure ice deposited at 100 K. The coverages of H_2O and N_2O_4 were 5 and 1.5 ML, respectively.

temperature cycling from disordered N_2O_4 layers, in which D-isomers are involved. Our IRAS measurements could not detect any evidence for $NO^+NO_3^-$ as well as D-isomers.

The interaction of free OH on amorphous ice with adsorbed NO_2 can be examined by IRAS. Figure 8 shows the difference spectra of IRAS before and after N_2O_4 adsorption on amorphous ice at 100 K, followed by annealing at the indicated temperatures. Positive bands represent band intensity reduction compared to a bare ice surface. The free OH band at 3700 cm^{-1} decreases in intensity upon NO_2 adsorption at 100 K. This intensity decrease is equal to the band intensity of free OH before NO_2 adsorption, indicating that all free OH interact with adsorbed N_2O_4 and, hence, they are present on the surface. In addition, the wide positive band centered at 3480 cm^{-1} indicates that bulk OH also interacts with adsorbed N_2O_4. Since the center frequency of this bulk OH band is ~100 cm^{-1} higher than the peak frequency of the amorphous bulk-ice OH band, H_2O interacting with N_2O_4 would be surface H_2O molecules that are weakly

(34) Givan, A.; Loewenschuss, A. *J. Chem. Phys.* **1990**, *93*, 7592.
(35) Givan, A.; Loewenschuss, A. *J. Chem. Phys.* **1991**, *94*, 7562.
(36) Schaff, J. E.; Roberts, J. T. *J. Phys. Chem.* **1996**, *100*, 14151.

bound to bulk ice. When the sample is heated at 115−120 K, the 3700 and 3480 cm^{-1} bands remain almost unchanged, indicating that the interaction of N_2O_4 with the ice surface is not changed at these temperatures. The change at 3230−3300 cm^{-1} is observed when amorphous ice is crystallized.

Returning to Figure 7, all the bands attributed to adsorbed N_2O_4 disappear when the sample is annealed at 140 K. However, this result does not imply the complete desorption of all NO_x species from the ice surface, since TDS after annealing at 140 K shows the desorption peak of chemisorbed NO_2 at ∼210 K (Figure 4). When NO_2 was dosed on the ice film at 130−140 K, no bands assignable to NO_x species were observed, but chemisorbed NO_2 was also observed in TDS. In coincidence with the TDS results, the IRAS band of chemisorbed NO_2 appears at 190 K and disappears at 230 K, as shown in Figure 7a. Part of the N_2O_4 adsorbed on the ice surfaces at <130 K, therefore, undergoes a conformational change at 140 K to form IRAS inactive configurations such as orientation c. Formation of this IRAS inactive species would result from formation of the H_2O-NO_2 adduct, which is decomposed at ∼185 K to produce gas phase H_2O (the β peak in TDS) and chemisorbed NO_2.

3.3. Thermal Decomposition of NO_2 in the Presence of Water−Ice. Wang et al.[19,20] reported that when NO_2 coadsorbed with H_2O on an Au(111) surface at <100 K, atomic oxygen was formed on the Au surface that functions as trapping sites. The atomic oxygen desorbed as molecular O_2 at ∼520 K during TPD. They concluded that this NO_2 decomposition is not due to the catalytic effects of an Au surface but attributable to the formation of D-isomers and their conversion to $NO^+NO_3^-$ on the ice surface. We also found that O_2 desorption occurs during TPD for NO_2 adsorbed on an ice film formed on Au(111). We have already reported that NO_2 chemisorbed on an Au(111) surface is partly decomposed at 180−240 K during TPD to produce NO and atomic oxygen on the surface.[23] The measured ratios of NO over NO_2 were 26% at 4.0 K s^{-1} of the TPD temperature ramp and 52% at 1.0 K s^{-1}.[22] This difference in NO ratio is due to the fact that the decomposition of chemisorbed NO_2 competes with its desorption. Although NO was thus produced during TPD, O_2 desorption was hardly observed at <600 K. However, after the adsorption−desorption cycle of chemisorbed NO_2 was repeated a few times at <400 K, O_2 desorption did occur at 507 K in TPD.[23] These results show that an Au(111) surface is intrinsically active for NO_2 decomposition to produce NO and atomic oxygen at temperatures as low as 200 K. Therefore, it is reasonably assumed that coadsorbed water enhances the adsorption and decomposition of chemisorbed NO_2 through H_2O-NO_2 adduct formation. Figure 7a shows that the 1171 cm^{-1} band appears at 190 K and disappears at 230 K. This band is assigned to chemisorbed NO_2 formed by the decomposition of the H_2O-NO_2 adduct. The band is broad and shifted to lower frequencies compared to the sharp 1182 cm^{-1} band of chemisorbed NO_2 that is directly formed from gas-phase NO_2. Both the broadening and the red shift of the band indicate strong interaction of chemisorbed NO_2 with the Au surface, which may lead to the NO_2 decomposition. Furthermore, TDS from N_2O_4/H_2O/Au(111) (Figure 4) shows that the β peak overlaps with the desorption peaks of NO_2 and NO. This implies that NO_2 formed by the decomposition of the H_2O-NO_2 adduct is dosed to the surface where the NO_2 decomposition is occurring. The overlapping of the β peak with the NO_2 desorption peak is essential for the decomposition of NO_2 on an Au surface, because NO_2 must be supplied to a catalytically active Au surface for its decomposition. Thus, coadsorbed water plays a role to make the NO_2 desorption temperature higher than the temperature for NO_2 decomposition on an Au surface by forming the H_2O-NO_2 adduct.

4. Conclusive Remarks

1. An amorphous ice film was prepared by deposition of gas-phase water on an Au(111) surface at <100 K, and a crystalline ice film was prepared at 140 K, followed by annealing at the same temperature for 10 min. The amorphous and the crystalline ice surfaces are characterized by rich and poor densities of free OH, respectively.

2. TDS from NO_2 adsorbed on amorphous and crystalline ice shows two H_2O desorption peaks at 157 and 185 K, the former being attributed to H_2O adsorbed on the Au surface and the latter to the decomposition of a H_2O-NO_2 adduct. The same TDS exhibits two NO_2 desorption peaks at 134 and 214 K, the former being ascribed to physisorbed N_2O_4 on the ice and the latter to NO_2 chemisorbed on the Au surface. Chemisorbed NO_2 is produced from the H_2O-NO_2 adduct. No difference between TDS features for amorphous and crystalline ice suggests that interaction of free OH with NO_2 is not related with formation of the NO_2-H_2O adduct.

3. IRAS shows that NO_2 is adsorbed as N_2O_4 with D_{2h} symmetry on crystalline and amorphous ice, and no other NO_x ($x = 1$, 2, and 3) species were detected. On crystalline ice, a disordered N_2O_4 layer is formed within ∼5 ML, while ordered N_2O_4 with its N−N bond axis perpendicular to the surface dominates at >5 ML. On amorphous ice, a new IRAS band of N_2O_4 is observed in the ONO symmetric stretching region but is not characterized well. N_2O_4 and/or NO_2 can reach the Au surface through the grain boundaries of a <10 ML crystalline ice film but cannot pass through the amorphous ice film even at 1 ML.

4. All free OH and part of the bulk OH interact with adsorbed $N_2O_4 \cdot H_2O$ molecules interacting with N_2O_4 would be surface H_2O molecules that are weakly bound to the bulk ice.

5. When NO_2 is coadsorbed with H_2O on Au(111), O_2 desorption occurred in TPD at ∼510 K. Since an Au(111) surface is catalytically active for NO_2 decomposition at 180−240 K, coadsorbed H_2O makes the NO_2 desorption temperature higher than 180 K by forming the H_2O-NO_2 adduct.

Acknowledgment. The authors thank Mr. Takehito Senga for his help in the present experiment.

LA000628N